Wireless Gait and Respiration Monitoring Using Nanocomposite Sensors

TAYLOR PIERCE, YUN-AN LIN and KENNETH J. LOH

ABSTRACT

The measurement of posture, loading conditions, and physiological parameters during physical activity is key in human performance monitoring and assessment. Of particular interest in this study is the monitoring of these parameters during high intensity activities associated with firefighting. The objective is to capture various walking cycles using nanocomposite pressure sensors built into the backpack-type harnesses of a Self-Contained Breathing Apparatus (SCBA) unit. It was hypothesized that the sensor's high stability, linearity, and sensitivity would allow this sensor to be used for human posture and activity monitoring. First, nanocomposite sensors were prepared by integrating piezoresistive graphene nanosheet thin films between elastomer layers. Two sensors were then integrated with the SCBA harnesses and mounted at symmetric locations to capture gait and respiration cycles. Second, a small, portable, wireless data acquisition unit was developed to non-intrusively monitor up to eight sensors and wirelessly transmit the data for external data storage and analysis. This sensing node included analog signal conditioning circuits alongside an ARM based microprocessor for analog to digital conversion, signal processing, and wireless transmission. Third, human participant tests were performed while wearing these harnesses. The participants performed various low intensity walking and respiratory cycles. The results confirmed that the wireless sensing unit was able to reliably acquire sensor measurements, while the sensing streams also exhibited unique features indicative of different activities and postures.

INTRODUCTION

Human kinematics monitoring is key to understanding, adapting, and improving human performance. Elderly care, injury rehabilitation, injury detection, and athletics

Taylor Pierce, University of California San Diego, Department of Electrical and Computer Engineering, Active, Responsive, Multifunctional, and Ordered-materials Research (ARMOR) Lab, 9500 Gilman Dr, La Jolla, CA 92093, USA.
Yun-An Lin and Kenneth J. Loh*, University of California San Diego, Department of Structural Engineering, ARMOR Lab, 9500 Gilman Dr MC 0085, La Jolla, CA 92093-0085, USA. * Corresponding author e-mail: kenloh@ucsd.edu

training all benefit from physical performance and physiological monitoring [1]. Traditionally, such monitoring has been accomplished through direct observation from a professional and direct feedback based on expertise. However, visual observations can be inaccurate and subjective, and the observer may not be able to see every detail. With continued advances in materials, electronics, and data processing, more and more sensors have started to enter the field in an attempt to broaden the availability and accuracy of human kinematic monitoring.

Among the diverse professions, achieving and maintaining high physical performance is crucial for emergency responders and, specifically, firefighters. The inherent nature of their profession exposes firefighters to extremely hazardous conditions. In fact, in 2020, an estimated 19,200 firefighter injuries were reported from fireground sites. Nearly 50% of these cases were because of overexertion or fall type injuries [2]. These injuries often occur in conditions with poor visibility, high stress factors, and during limited communication. As such, an emphasis on extensive training and simulation has been taken to minimize the potential for injury. However, these situations create significant difficulties in direct observational monitoring and feedback, even when they are performed in a controlled training environment.

To expand on the ability for key decision makers to observe active firefighters, a system is proposed to continuously monitor and report the kinematics of these firefighters. According to the previously reported injury cases, respiration and gait monitoring were targeted based on their reported ability to identify fatigue and fall conditions [3-5]. A number of existing technologies were analyzed for use in these applications. Existing sensors for high intensity activity monitoring typically include inertial measurement units (IMUs), marker-based motion capture, or surface electromyography (EMG) sensors. Commercial wearable sensors utilizing IMUs have been leveraged for gait monitoring ([6]) but have been noted for inaccurately capturing these signals [7]. Motion capture naturally require setup conditions and visibility conditions that would not be feasible in firefighting situations. Surface EMG sensors are typically extremely sensitive to motion artifacts and skin conditions [8], making them difficult to adapt for firefighting and physically intensive scenarios.

The objective of this work was to develop a system capable of capturing gait and respiration signals without impeding movement or dressing routines of responding firefighters. To overcome the challenges previously presented, nanocomposite pressure sensors were developed and integrated with existing Self-Contained Breathing Apparatus (SCBA) harnesses. In addition, a customized, portable, wireless miniaturized data acquisition (DAQ) unit was developed to capture and report these signals in real-time.

EXPERIMENTAL DETAILS

Wireless Sensing Node

A customized wireless sensing node or data acquisition (DAQ) node was developed for aggregating wearable sensor data and streaming them in real-time to a remote base station (Figure 1). At the heart of the computational core was a Texas Instruments CC1350 microcontroller (mcu). This microcontroller operates at approximately 51 μA/MHz, or 2.5 mA at full 48 MHz operation. This microcontroller

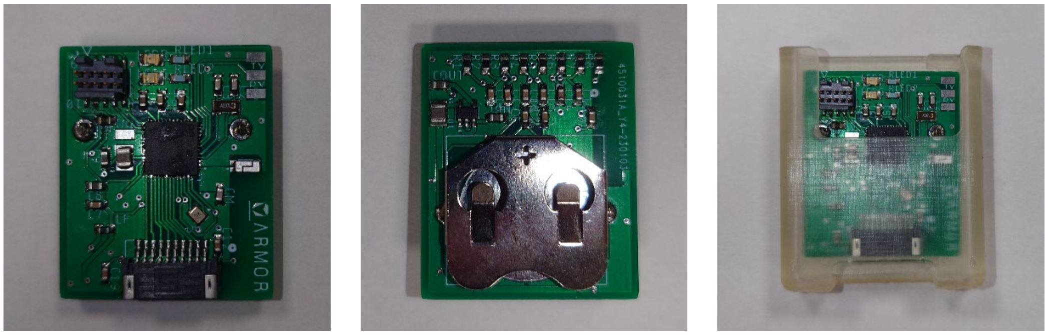

(a) (b) (c)

Figure 1. The (a) top and (b) bottom view of the wireless DAQ, as well as when it is inserted in its (c) 3D-printed enclosure, are shown.

also includes several key functions for this DAQ on-chip, including a 12-bit analog-to-digital converter (ADC) with up to 8-pin multiplexing and a 2.4 GHz wireless transceiver for Bluetooth low energy (BLE) transmission (Figure 1a).

Up to eight sensors could be interfaced with this wireless DAQ. Sensor impedance measurements were captured using a basic voltage divider circuit, with a parallel capacitor to create an analog ~ 4 kHz filter in order to reduce aliasing effects. The 12-bit ADC utilized an on-board 4.3 V reference voltage to achieve a voltage resolution of ~ 1 mV. The mcu was configured with an ADC sampling period of 682 μs, sequentially multiplexed across 8 channels and a 12 ms delay between sampling to avoid overloading the transceivers, which resulted in a per-channel sampling rate of ~ 60 Hz. The actual measured sample rate was somewhat variable because of lost or corrupted packets or other mcu computations. Additional components for the wireless sensing node included a battery retainer for a CR2032 coin cell battery, power regulation, and a chip antenna (Figure 1b). This resulted in a customized DAQ board capable of sampling up to eight channels continuously for several hours. The wireless transmission range was estimated to be ~ 10 m. Finally, the DAQ board was inserted in a custom, 3D-printed, protective exterior housing (Figure 1c).

Pressure Sensors

Nanocomposite wearable pressure sensors were fabricated for integration with an SCBA harness. The pressure sensor developed for this study was of a sandwich structure, where a piezoresistive thin film rested between two layers of Dragon Skin™ elastomer (Figure 2). By incorporating a piezoresistive thin film within a deformable soft material, the Dragon Skin™ would deform in response to applied pressure to induce strain in the strain-sensitive thin film, which causes its electrical resistance to change accordingly.

The fabrication process of the pressure sensor was as follows. First, a layer (~ 3 mm thick) of Dragon Skin™ was casted and cured in a small weighing dish. Second, a strip of 3M Tegaderm film was laid onto the cured Dragon Skin™ elastomer. The purpose of the 3M Tegaderm film was to introduce a smooth, hydrophilic surface that permitted the deposition of the sensing element later. Before depositing the film, two-point probe electrodes were formed by painting two small rectangular strips of Voltera flexible silver trace. The silver pads were allowed to dry in room temperature

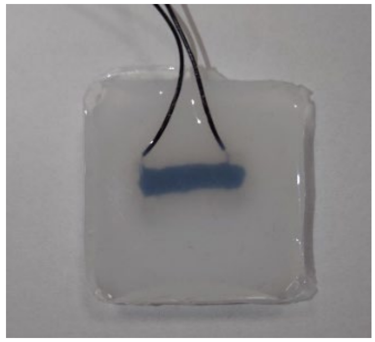

Figure 2. The nanocomposite pressure sensor is based on a piezoresistive thin film sandwiched between two elastomer layers.

before a thin multi-strand wire was soldered to each of the electrode pads. Third, three layers of nanocomposite ink was drop casted to form a piezoresistive thin film between the two electrodes. Care was taken to ensure that good contact with the electrodes was made. The thin film was a graphene nanosheet (GNS) and ethyl cellulose (EC) nanocomposite, and its detailed fabrication method was presented by Lin *et al.* [9]. Last and upon drying of the nanocomposite, a top layer of Dragon Skin™ (~ 3 mm thick) was casted and cured to obtain the pressure sensor.

Pressure Sensor Characterization

Prior to affixing the wearable pressure sensors to the SCBA, a series of sensor characterization tests were conducted in the laboratory. For these tests, each pressure sensor was placed on a flat surface, and calibration masses (*i.e.*, 10 g, 50 g, 100 g, and 200 g) were placed at the center of the pressure sensor and directly over where the piezoresistive nanocomposite was located. Sensor electrical resistance values were recorded for each case using a Keysight 34461A digital multimeter.

Sensor Integration with SCBA

The wearable nanocomposite pressure sensors were fabricated and then integrated at two locations on the SCBA harness, one on each harness strap. These sensors were mounted along the frontmost contact position of the harness strap, between the strap and sternum, as are depicted in Figure 3. Each pressure sensor was temporarily affixed to the harness strap using self-adhesive athletic tape. A temporary attachment of the pressure sensors was preferred so that the SCBA harness unit could be reused for different tests not discussed in this work.

On the other hand, the wireless sensing node was mounted at the top of the empty oxygen tank. This location was chosen to minimize radio frequency interference from the equipment and subject while maintaining good line-of-sight between the wireless sensing node and the base station. The multi-strand wires of each pressure sensor were routed along the harness strap and plugged directly into the wireless DAQ.

Human Participant Tests

A series of human participant tests were conducted to evaluate the pressure sensors' ability to record unique sensing streams associated with different physical

(a) (b)

Figure 3. (a) Subjects wore the SCBA unit during testing, where (b) pressure sensors were integrated with the SCBA harness.

activities. The human subject study was approved by the University of California San Diego, Institutional Review Boards (IRB), Human Research Protection Program, under Project No. 806354, and informed written consent was obtained from all participants. Two types of activities were chosen to demonstrate differential loading movements versus symmetric loading movements. First, for differential type movements, pressure peaks were expected to alternate between the left and right harness straps. To generate this behavior, the subject walked in a circle in both clockwise and counterclockwise directions. In addition, the subject performed these movements first at a slow pace, before walking at a normal, casual pace. Second, for symmetric type movements, pressure was expected to be approximately evenly distributed between the straps and in unison. Here, the subject maintained a relaxed and stationary standing position while taking slow deep breaths. Throughout each test trial, the wireless sensing node streamed the pressure sensor data in real-time to a personal computer connected through a reference CC1350 Launchpad board.

RESULTS AND DISCUSSION

As mentioned earlier, human participant tests were conducted in accordance with the University of California San Diego IRB Project No. 806354. Pressure sensor data were acquired using the wireless sensing node. A basic outlier filter was implemented to remove corrupted data points, if any, resulting from the wireless transmission process. All the data presented in this work was normalized with respect to a baseline measurement captured from the initial few moments of each test procedure.

Nanocomposite Pressure Sensor Response

Prior to human participant testing, the response of the nanocomposite pressure sensors was characterized using calibrated weights. The applied pressure values (P) were calculated from the dimensions of the calibration masses (*i.e.*, contact area, A) and the established mass (w), where $P=w/A$. In addition, normalized pressure was

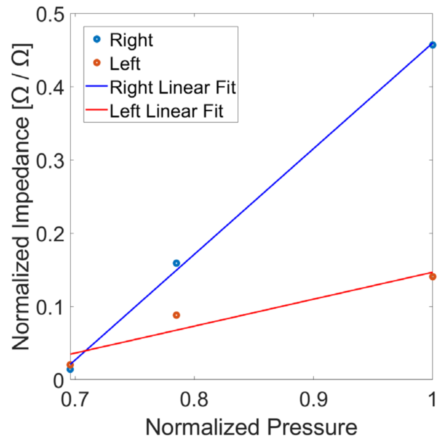

Figure 4. The normalized impedance results of two wearable pressure sensors (*i.e.*, "Right" and "Left") are plotted with respect to normalized pressure.

calculated by dividing the contact pressure of each case by the maximum pressure applied (*i.e.*, using the 200 g mass). A set of representative results for two sensors (*i.e.*, labeled as "Right" and "Left") are shown in Figure 4. The sensors failed to exhibit any noticeable change in its electrical resistance for the 10 g mass case, so the results were excluded in Figure 4. For the other masses, the sensors all exhibited significant changes in normalized impedance. Calibration tests first demonstrated a minimum threshold force for the sensors as the 10g mass failed to measurably impact the impedance of the sensor. In fact, sensor linearity for the subsequent three masses was exceptional, with R^2 values of 0.999 for the "Right" sensor and 0.908 for the "Left" sensor. Sensitivity differences (*i.e.*, slopes of the linear fit) varied because of experimental error during manual fabrication of the piezoresistive sensing elements.

Gait Monitoring

Human participant tests were performed with the participant wearing the SCBA harness unit. The subject walked at different paces and in both clockwise and counterclockwise directions. A representative set of results for the subject walking slowly in the counterclockwise and clockwise directions are shown in Figure 5a and 5b, respectively. The results for the normal walking pace are shown in Figure 6.

These gait monitoring results showed a distinct, asymmetric loading of the shoulder straps as a result of the weight of the tank shifting between the left and right sides of the body during walking. Similar to the previous sensor characterization tests, sensitivity differences were identified between the Right and Left sensors, though imperfect loading and sensor placement likely factored into this discrepancy as well. A frequency analysis was performed on these datasets and showed a dominant frequency of 0.268 Hz, 0.259 Hz, 0.616 Hz, and 0.474 Hz for slow counterclockwise walking, slow clockwise walking, normal counterclockwise walking, and normal clockwise walking, respectively. These results matched the pace at which the participant walked during testing.

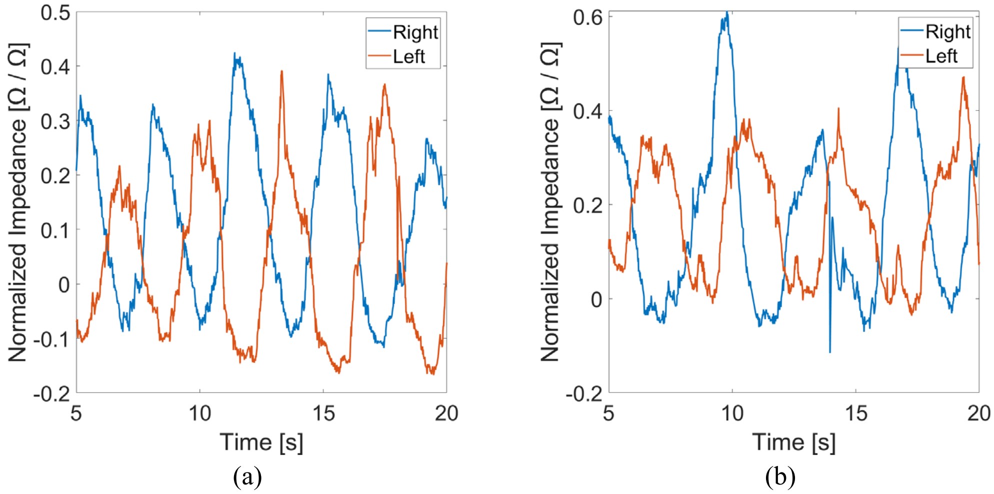

Figure 5. A 15 s segment of the pressure sensor data when the participant walked slowly in the (a) counterclockwise and (b) clockwise directions are plotted.

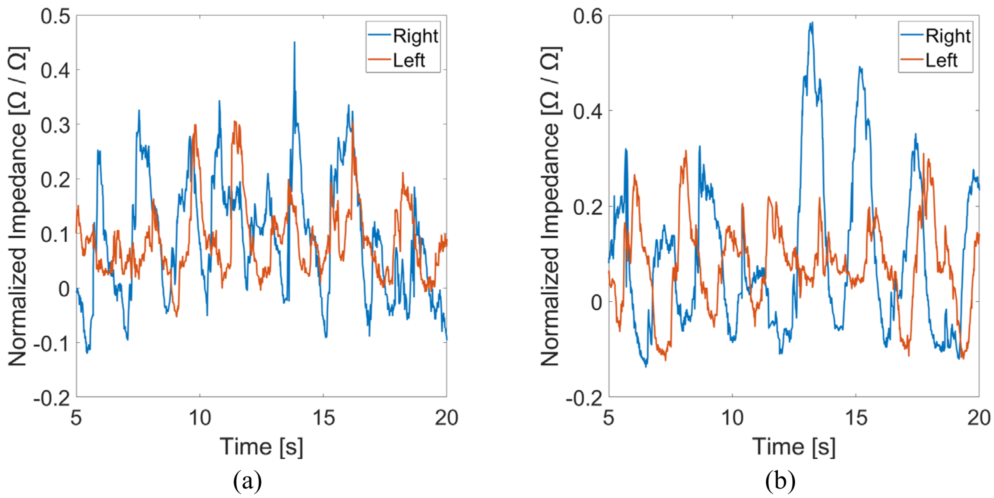

Figure 6. A 15 s segment of the pressure sensor data when the participant walked at a normal pace and in the (a) counterclockwise and (b) clockwise directions are plotted.

Respiration

Respiration and, specifically, deep breathing tests were performed, and the data from the sensors are presented in Figure 7. Distinct symmetric pressure peaks were identified at steady rates. From spectral analysis, a dominant frequency of 0.170 Hz was identified, predicting a respiration rate of 10 breaths/min, which was consistent with experimental observations. Sensor sensitivity differences were also observed.

CONCLUSIONS

Graphene-elastomer pressure sensors, which were connected to a customized wireless sensing node, were integrated with an SCBA harness. Human participant studies confirmed that this system could capture unique and identifying waveforms associated with gait and respiration. It is proposed that such a system could be utilized in active firefighting to aid in determining their fatigue, overall health, and the types

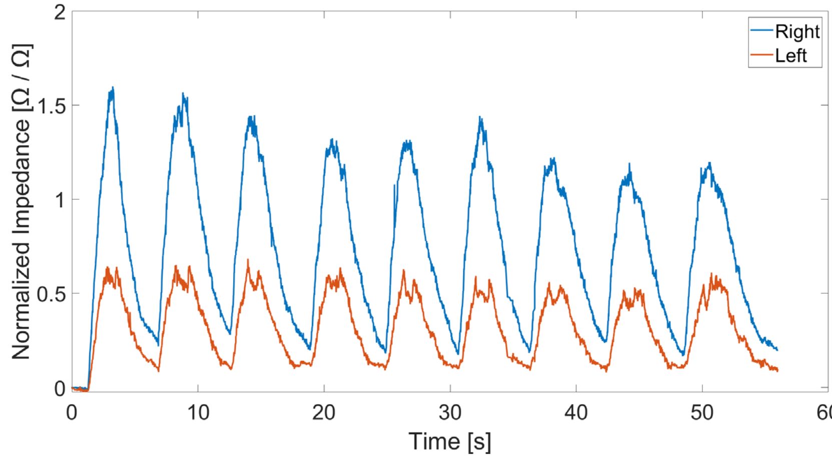

Figure 7. The pressure sensors' normalized impedance changes were captured during deep breathing tests.

of activities they are engaged with during emergency response scenarios. Future work will consider a greater variety of physical activities to further validate the system.

ACKNOWLEDGEMENTS

The research was supported by the U.S. Office of Naval Research (ONR) under grant numbers N00014-20-1-2329 and N00014-22-1-2591.

REFERENCES

1. Mukhopadhyay, S. C. 2015. "Wearable Sensors for Human Activity Monitoring: A Review," *IEEE Sensors Journal*, 15(3): 1321-1330
2. Campbell, R. B., B. Evarts, and J. L. Molis. 2020. "United States Firefighter Injuries in 2019," National Fire Protection Association, Research, Data and Analytics Division.
3. Zhou, L., C. Tunca, E. Fischer, C. M. Brahms, C. Ersoy, U. Granacher, and B. Arnrich. 2020. "Validation of an IMU Gait Analysis Algorithm for Gait Monitoring in Daily Life Situations," presented at the 42nd Annual International Conference of the IEEE Engineering in Medicine & Biology Society (EMBC), Montreal, QC, Canada, July 20-24, 2020.
4. Vanegas E, R. Igual, and I. Plaza. 2020. "Sensing Systems for Respiration Monitoring: A Technical Systematic Review," *Sensors*, 20(18): 5446.
5. Lin, Y-A., E. Noble, C-H. Loh, and K. J. Loh. 2022. "Respiration Monitoring using a Motion Tape Chest Band and Portable Wireless Sensing Node," *Journal of Commercial Biotechnology*," 27(1).
6. Zhuang, Z. and Y. Xue. 2019, "Sport-Related Human Activity Detection and Recognition Using a Smartwatch," *Sensors*, 19(22): 5001.
7. Storm, F. A., B. W. Heller, and C. Mazzà. 2015. "Step Detection and Activity Recognition Accuracy of Seven Physical Activity Monitors," *PLoS one*, 10(3): e0118723.
8. Campanini, I., A. Merlo, C. Disselhorst-Klug, L. Mesin, S. Muceli, and R. Merletti. 2022. "Fundamental Concepts of Bipolar and High-Density Surface EMG Understanding and Teaching for Clinical, Occupational, and Sport Applications: Origin, Detection, and Main Errors," *Sensor*s, 22(11):4150.
9. Lin, Y-A., Y. Zhao, L. Wang, Y. Park, Y-J. Yeh, W-H. Chiang, and K. J. Loh. 2021. "Graphene K-Tape Meshes for Densely Distributed Human Motion Monitoring," *Advanced Materials Technologies*, 6(1): 2000816.